35th Annual International Conference of the IEEE EMBS
Osaka, Japan, 3 - 7 July, 2013

Effects of the Air Sac Thickness on Ventilation by a 1D Model of an Avian Respiratory System*

Akira Urushikubo, Masanori Nakamura, and Hiroyuki Hirahara

Abstract— **Airflow in an avian respiratory system was simulated to study why birds affected with airsacculitis have respiratory distress. The airflow in the avian lung was modeled with a 1D electrical circuit and simulated for investigating what effect an increase in wall thickness of air sacs caused by airsacculitis has on flow in lung. The results demonstrated that thickening of the air sac wall caused anti-synchronization between an elastic recoiling force of the air sac walls and an intra-pleural pressure, bringing difficulties in expansion of air sacs to draw in airs during an inspiration period and thereby decreasing air to be pumped out during an expiration period. This was reflected in a decrease in air flow volume in parabronchi where gas exchange takes place. Therefore, it was concluded that airsacculitis causes imbalance in air flow dynamics in the avian lung and thus impairs breathing ability of birds.**

I. Introduction

It is known that birds have more efficient respiratory system than other species to keep performing flapping flight at high altitudes over a long period of time [1], [2]. To date, two factors, namely, airway structure and air sacs, are considered to achieve such efficient respiration [3].

The air sacs are stretchy bags composed of thin membranes [4], [5]. They deform largely and repeatedly in accordance with a change in pleural pressure to store in and push out air for helping continuous flow in parabronchi where exchange of oxygen and carbon dioxide takes place [6].

Airsacculitis is one of air sac diseases stemming from mycoplasmal disease. Once affected, the air sac wall is thickened [7]. It is also known that birds infected with airsacculitis exhibit respiratory distress [8]. Considering these two facts together, we postulate that the changes in mechanical or material properties of air sacs by airsacculitis would affect flow dynamics within the respiratory system to lead respiratory distress.

The present study is aimed to investigate effects of thickness of air sac walls on flow in the parabronchi for understanding why birds affected with airsacculitis have respiratory distress.

*This research is supported by the Sekisui Chemical Grant Program for Research on Manufacturing Based on Innovations Inspired by Nature.

A. Urushikubo is with Department of Mechanical Engineering, Saitama University, Shimo-Okubo 255, Sakura, Saitama, Japan (e-mail: s12mh103@mail.saitama-u.ac.jp).

M. Nakamura is with Department of Mechanical Engineering, Saitama University (phone and fax: +81-48-858-3443; e-mail: masanorin@mech.saitama-u.ac.jp).

H. Hirahara is with Department of Mechanical Engineering, Saitama University (e-mail: hhira@mail.saitama-u.ac.jp)

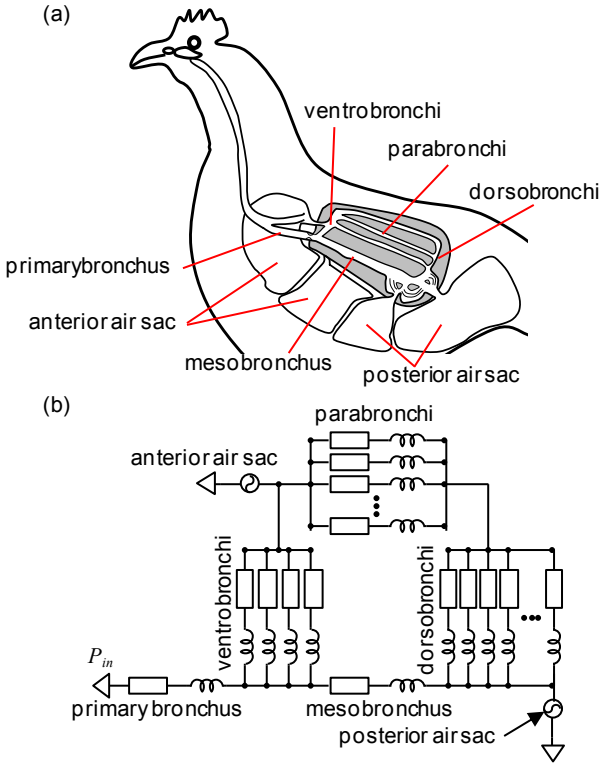

Figure 1. 1D electrical circuit model of an avian respiratory system

II. Method

A. 1D Electrical Circuit Model of an Avian Respiratory System

Fig. 1 (a) presents a schematic drawing of an avian lung. The respiratory system starts from a primary bronchus that is connected to the syrinx, the trachea and the pharyngeal portion. The primary bronchus divides into ventrobronchi going upward and mesobronchus going rightward. The mesobronchus turns around and is connected to ventrobronchi via dorsobronchi and parabronchi, forming a looped structure. Air sacs are present in both anterior and posterior sides, attached to air ways. Fig. 1 (b) illustrates the 1D electrical circuit model of an avian respiratory system. Resistance and inductance of each airway were expressed by a resistor and an inductor. Energy and momentum losses due to branching of airways were neglected. Airway compliances were also ignored, since a volume change of the lung during a respiratory cycle was limited to only 1.4 % [9]. In reality, more than one air sac is present in each side, but here grouped together and represented by one air sac in each. A temporal variation of pressure within an air sac was represented by a

pressure source.

Assuming that a flow in an avian respiratory system is laminar and can be described by the Hagen-Poiseulle law, a flow resistance R and inductance L are expressed [10] by

$$R = \frac{128\mu l}{\pi D^4} \tag{1}$$

$$L = \frac{4\rho l}{\pi D^2} \tag{2}$$

where μ is a dynamic viscosity of air, l and D are the length and diameter of an airway, and ρ is a density of air.

In reference to the data of domestic fowl (*gallus domesticus*) [11], [12], we established 4 ventrobronchi, 15 dorsobronchi and 500 parabronchi in the model. The radius, length and number of bronchi are summarized in Table 1. These data were determined from [11]-[14]. Since airways are present in parallel, their resistance and inductance were totaled for each by simply taking the sum of the inverses of the individual resistances and inductances.

B. Air Sac Model

In an inspiratory period, an intra-pleural negative pressure becomes negative to inflate air sacs. As a result, a pressure within the air sacs also becomes negative, thereby allowing air to flow in the air sacs. In contrast, during an expiratory period, air sacs recoil by elastic force to squeeze air to airways. Throughout a respiratory period, a pressure within an air sac, P_{AS}^k, an elastic force in wall of the air sac, τ^k, and an intra-pleural pressure, P_P, are mechanically balanced;

$$P_{AS}^k = P_P + \tau^k \tag{3}$$

where superscript k stands for the group of air sacs, anterior or posterior. Assuming that the air sac behaves like a rubber sphere, the elastic force in the air sac wall was expressed by

$$\tau = \frac{E}{2(1+\nu)}\left\{2\left(\frac{r_0+\delta}{r+\alpha\delta}-\frac{r_0}{r}\right)+\frac{1}{2}\left(\frac{(r_0+\delta)^4}{(r+\alpha\delta)^4}-\frac{r_0^4}{r^4}\right)\right\} \tag{4}$$

where E is the Young's modulus, ν is the Poisson ratio, r_0 and r are an internal radius at a natural state and at time t, respectively, δ is thickness of the air sac wall, and α is a change ratio of the wall thickness [15]. Although superscript k exists in all variables of eq. (4), it is omitted here for clarity.

The initial radius r_0 of an air sac is gained from

$$r_0^{\,k} = \sqrt[3]{\frac{3}{4\pi}V_0^{\,k}} \tag{5}$$

where V_0 is the volume of air sac at the natural state. Similarly, the radius of the air sac at time t is obtained from

$$r^k = \sqrt[3]{\frac{3}{4\pi}\left(V_0^k + \Delta V^k\right)} \tag{6}$$

where ΔV^k is an increment in the volume of air sac k from the natural state. It is calculated by an integration of flow q going in and out from the air sac,

TABLE 1 RADIUS, LENGTH, NUMBER OF BRONCHI

Name	*r* [mm]	*l* [mm]	*NB*
Primary bronchus	2.25	12	1
Mesobronchus	2.25	30	1
Dorsobronchi	1.5	16	15
Parabronchi	0.5	40	500
Ventrobronchi	1	16	4

r: Radius, *l*: Length, *NB*: Number

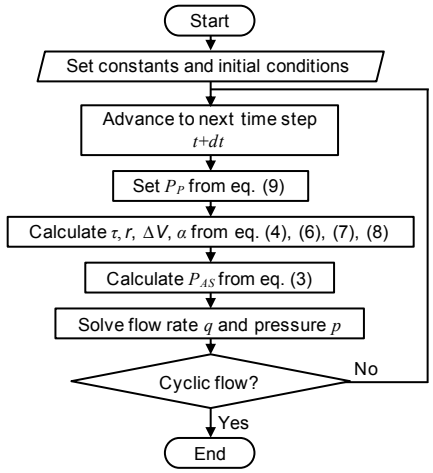

Figure 2. A flowchart of the avian respiratory flow simulation in combination with the mechanical model of air sacs.

$$\Delta V^k = \int_0^t q^k(t)dt\ . \tag{7}$$

Considering incompressibility of the air sac wall, we establish the following equation

$$(\delta\cdot\alpha)^3 + 3r(\delta\cdot\alpha)^2 + 3r^2(\delta\cdot\alpha) - \left\{(r_0+\delta)^3 - r_0^{\,3}\right\} = 0 \tag{8}$$

to obtain the change ratio of the wall thickness, α.

C. Simulation Conditions

It is assumed that air flow is an incompressible fluid with a density ρ of 1.2 kg/m^3 and a dynamic viscosity μ of 1.82×10^{-5} Pa·s. Assuming sinusoidal respiration, we gave an intra-pleural pressure P_P as

$$P_P = P_0\sin(2\pi ft) \tag{9}$$

where P_0 is a pressure amplitude and f is a respiratory frequency. Since respiratory distress becomes more vital in exercise, the panting breath condition was used. In reference to Calder and Schmidt-Nielsen [16], the respiratory frequency of 10 Hz was used. The pressure amplitude P_0 of 10 Pa was given such that a tidal volume obtained by simulations was equal to the one measured by Calder and Schmidt-Nielsen [16]. The volume of anterior and posterior air sacs at the natural state are set such that $V^{ante} = 97.15\times10^{-6}$ m^3 and $V^{post} = 101.4\times10^{-6}$ m^3 from a total volume of air sacs in anterior and posterior groups [17]. In reference to biological tissues, the Young's modulus of the air sac was 1 MPa, and the Poisson's

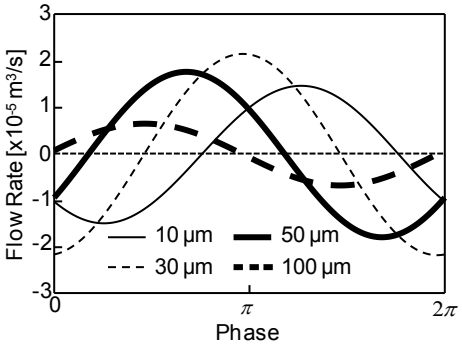

Figure 3. Temporal variation of the flow rate in the parabronchi

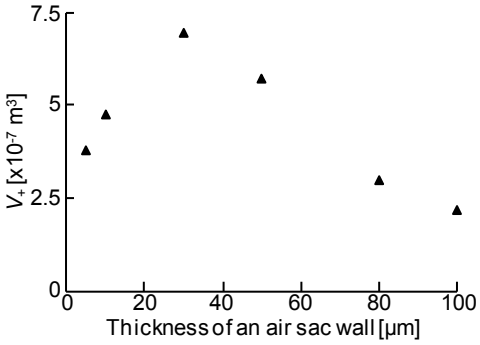

Figure 4. Plot of the forward flow volume during one respiratory cycle against the wall thickness of air sacs

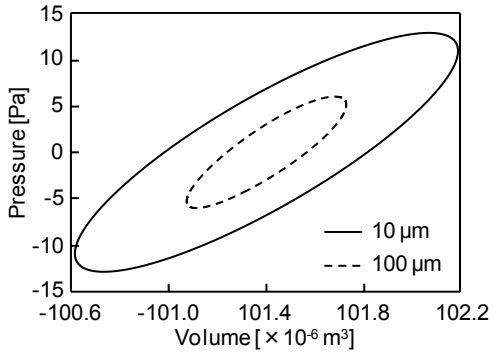

Figure 5. Pressure-volume diagrams of air sacs with the wall thickness of 10 μm and 100 μm

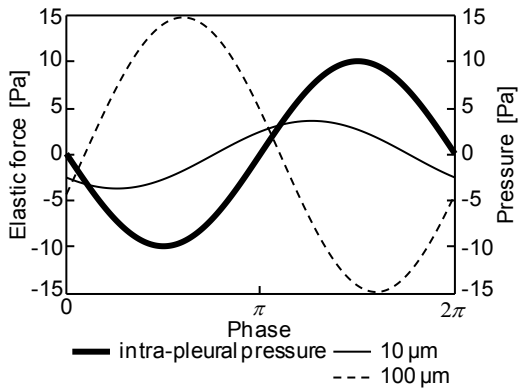

Figure 6. Temporal variation of the elastic force of the posterior air sacs with the wall thickness of 10 μm and 100 μm along with that of intra-pleural pressure

ratio v was set to be 0.5. The thickness δ was varied from 5 μm to 100 μm to see its effects on respiratory flow.

D. Simulation Procedure

A flowchart of the simulation is shown in Fig. 2. The simulation was commenced from a quiescent flow state, at which air sacs were assumed to be in a natural state. With advancement of a time step, an intra-pleural pressure P_P was set from eq. (9), and elastic forces of the air sacs τ^{ante} and τ^{post} were calculated to obtain pressures in the air sacs, P_{AS}^{ante} and P_{AS}^{post}. Provided P_{AS}^{ante} and P_{AS}^{post} as pressure boundary conditions at air sacs with P_{in}=0 Pa at the inlet, flow in an avian respiratory circuit was simulated by solving equations of the model schematically presented in Fig. 1(b). This process was repeated until cyclically repeatable flow was obtained. In actual simulations, a time increment of 1×10^{-5} s was used. The repeatability was attained at the 8th cycle when a relative error between cycles was smaller than 0.5%.

III. RESULTS

A temporal variation of flow in patabronchi is shown in Fig. 3. In this figure, solid, broken, thick and thick-solid lines represent data with the air sac thickness of 10, 30, 50 and 100 μm. A flow from the posterior side to the anterior side is defined as a forward direction, and expressed in a positive value. Fig. 3 demonstrates that the flow in the parabronchi varies sinusoidally with time. In any wall thickness of air sacs, the flow exhibited both positive and negative values. In other words, a flow in the parabrochi was bidirectional in any cases.

A total volume of the flow that has passed in the forward direction of parabronchi during one respiratory cycle was assessed as V^+ in each condition. The value of V^+ is plotted against the thickness of air sacs in Fig. 4. This shows that the value of V^+ became larger with an increase in wall thickness of the air sac, but turned into a decrease after maximum value at the wall thickness of 30 μm and decayed drastically with a further increase in the wall thickness.

A pressure-volume relation of the posterior air sac with the air sac wall thickness of 10 μm (solid line) is compared with that of 100 μm (broken line) in Fig. 5. The horizontal axis represents the volume of an air sac and the vertical axis does a pressure within the air sac. As seen, the area encompassed by the pressure-volume curve at the air sac thickness of 10 μm was larger than that at the air sac thickness of 100 μm. Other conditions included, the area encompassed by the pressure-volume curve decreased with an increase in the wall thickness. A similar characteristic was found in pressure-volume relations of the anterior air sac.

Fig. 6 plots a time variation of elastic forces of the posterior air sac with the wall thickness of 10 μm (solid line) and 100 μm (broken line). A time variation of the intra-pleural pressure (thick line) is also presented. As demonstrated, the elastic force of the posterior air sac with the wall thickness of 10 μm almost synchronized with the intra-pleural pressure, whereas that of 100 μm did not.

IV. Discussion

In the present study, an avian respiratory flow was simulated using the 1D electrical circuit model of an avian respiratory system combined with the mechanical model of air sacs. As seen in Fig. 4, the increase in wall thickness of air sacs induced a decrease in the flow volume in parabronchi where gas is exchanged. Since the flow volume passing through the parabronchi is directly associated with a rate of gas exchange or a respiratory function, the results obtained by the simulation would demonstrate that the increase in wall thickness of air sacs actually caused respiratory distress as seen in natural birds affected with airsacculitis.

An intra-pleural pressure works to compress air sacs to expel air when positive, whereas it helps enlarge air sacs to suck air when negative. Meanwhile, Eq. (4)-(8) describe that an increase in an air sac volume decreases thickness of the air sac wall and generates an elastic force to shrink the air sac. For those, synchronization of the elastic force of air sacs and the intra-pleural pressure is necessary to facilitate inflation and deflation of air sacs. As demonstrated in Fig. 6, an increase in the wall thickness of air sacs caused phase shifting of the elastic force of air sacs against the intra-pleural pressure. As a result, the elastic force of air sacs is in anti-phase with the intra-pleural pressure when the air sac wall is thickened. This means that even if intra-pleural pressure is increased to promote expiration of air sacs, they do not follow it and do not work. This is manifested in Fig. 5 showing that the area encompassed by the pressure-volume curve, or the work, decreased with thickening of the air sac wall. Therefore it was suggested that thickening of the air sac wall occurring in birds affected with airsacculitis caused anti-synchronization between an elastic recoiling forces of the air sac walls and an intra-pleural pressure, bringing difficulties in expansion of air sacs to draw in airs during an inspiration period and thus decreasing air to be pumped out to airways during an expiration period. As a consequence, a flow volume passing though the parabronchi where gas exchange takes place decreased as shown in Fig. 4, and birds go into respiratory distress. Thus, the respiratory distress caused by airsacculitis results from the total impairment of the flow system in avian lungs.

It is generally considered that, in real birds, air flows unidirectionally in parabronchi during both inspiration and expiration. This unidirectional flow in the parabronchi is considered to be beneficial for efficient gas exchange [2], [6]. However, it was not observed in any conditions in the present study. This would be due to usage of 1D model in which airway structure is not taken into consideration. In fact, the analysis using three dimensional flow channel of an avian respiratory system demonstrated that the flow structures, like vortices, help achieve the unidirectional flow in parabronchi [18]. In future studies, we will perform a three dimensional analysis of flow dynamics in combination with the air sac model proposed here to confirm the present findings.

V. Summary and Conclusion

The airflow in the avian lung was numerically studied with a 1D electrical circuit to understand study why birds affected with airsacculitis have respiratory distress. The results suggested that thickening of the air sac wall occurring in birds affected with airsacculitis resulted in a phase mismatch between an elastic recoiling force of the air sac walls and an intra-pleural pressure, bringing difficulties in efficient inflation and deflation of air sacs and thereby decreasing the flow in parabronchi. Therefore, it was concluded that impairment of breathing of birds affected with airsacculitis is caused by an imbalance in air flow dynamics in the avian lung due to dysfunctional movements of air sacs.

Acknowledgment

The authors acknowledge the Sekisui Chemical Grant Program for Research on Manufacturing Based on Innovations Inspired by Nature for funding this research.

References

[1] V. Tucker, "Respiratory physiology of house sparrows in relation to high-altitude flight," J. Exp. Biol., vol. 48, pp. 55-66, 1968.
[2] K. Schmidt-Nielsen, "Animal Physiology; Adaptation and environment," 5th ed. University of Tokyo Press, Tokyo, 2007, pp. 37-42, (in Japanese).
[3] D. Kuethe, "Fluid mechanical valving of air flow in bird lungs," J. Exp. Biol., vol. 136, pp. 1-12, 1988.
[4] P. W. Gilbert, "The avian lung and air-sac system," Auk, vol. 56, pp. 57-63, 1939.
[5] M. R. Fedde, "Relationship of structure and function of the avian respiratory system to disease susceptibility," Poult. Sci., vol. 77, pp. 1130-1138, 1988.
[6] P. Scheid and J. Piiper, "Respiratory mechanics and air flow in birds," in Form and Function in Birds, vol. 4, A. S. King and J. McLelland, Ed. London: Academic Press, 1989, pp. 369-391.
[7] O. J. Fletcher, S. E. Fairchild, F. G. Smith and D. P. Trampel, "Histology of air sac lesions induced in chickens by contact exposure to mycoplasma synoviae," Vet. Pathol., vol. 13, pp. 303-314, 1976.
[8] B. P. Shankar, "Common respiratory diseases of poultry," Vet. World., vol. 1, no. 7, pp. 217-219, 2008.
[9] J. H. Jones, E. L. Effmann and K. Schmidt-Nielsen, "Lung volume changes during respiration in ducks," Respir. Physiol., vol. 59, pp. 15-25, 1985.
[10] L. H. van der Tweel, "Some physical aspects of blood pressure, pulse wave, and blood pressure measurements," Am. Heart J., vol. 53, pp. 4-17, 1957.
[11] A. R. Akester, "The comparative anatomy of the respiratory pathways in the domestic fowl (Gallus domesticus), pigeon (Columba livia) and domestic duck (Anas platyrhyncha)," J. Anat., vol. 4, pp. 487-505, 1960.
[12] A. S. King, "Structural and functional aspects of the avian lungs and air sacs," Int. Rev. Gen. Exp. Zool., vol. 2, pp. 171-267, 1966.
[13] A. Makanya, V. Djonv, "Development and spatial organization of the air conduits in the lung of the domestic fowl, Gallus gallus variant domesticus," Microsc. Res. Tech., vol. 71, pp. 689-702, 2008.
[14] B. Onuk, M. Hazitoglu, M. Kabak, "Gross anatomy of the respiratory system in goose (Anser anser domesticus): Bronchi and sacci pneumatici," Vet. J. Ankara Univ., vol. 56, pp. 165-170, 2009.
[15] R. Kubo, "Large elastic deformation of rubber," J. Phys. Soc. Jpn., vol. 3, pp. 312-317, 1948.
[16] W. Calder, K. Schmidt-Nielsen, "Temperature regulation and evaporation in the pigeon and the roadrunner," Am. J. Physiol., vol. 213, pp. 883-889, 1967.
[17] A. S. King and D. C. Payne, "The maximum capacities of the lungs and air of Gallus domesticus," J. Anat. Lond., vol. 96, pp. 495-503, 1962.
[18] J. N. Maina, P. Singh, E. Moss, "Inspiratory aerodynamic valving occurs in the ostrich, struthio camelus lung: A computational fluid dynamics study under resting unsteady state inhalation," Respir. Physiol. Neurobiol., vol. 169, pp. 262-270, 2009.